

## Transient field at nitrogen nuclei recoiling in iron and the magnetic moment of the $^{15}\text{N}$ first excited state

M. Forterre, J. Gerber, and J. P. Vivien  
*Centre de Recherches Nucléaires, Strasbourg, France*

M. B. Goldberg,\* K.-H. Speidel, and P. N. Tandon†  
*Institut für Strahlen- und Kernphysik, Bonn, Germany*  
 (Received 21 January 1975)

Precession measurements have been performed on nuclear-excited nitrogen ions recoiling in magnetized iron employing the implantation perturbed-angular-correlation technique. The transient magnetic field, calibrated with the  $^{16}\text{N}(1^-)$  state, was found to be enhanced by a factor of 2.1(5) over the empirically adjusted Lindhard-Winther prediction. A negative sign was determined for this  $g$  factor and a value of  $g = +0.9(3)$  for that of the  $^{15}\text{N}(\frac{5}{2}^+)$  state.

[ NUCLEAR REACTIONS  $^{13,14}\text{C}({}^3\text{He}, p)$ ,  $E_{{}^3\text{He}} = 2-4$  MeV; measured  $W(\theta_\gamma)$   $^{15,16}\text{N}$  levels, recoil in magnetized iron, deduced  $H_{\text{transient}}$ ,  $g$ . ]

### I. INTRODUCTION

The existence of a magnetic field at the nucleus during the slowing-down process in ferromagnetic media was originally demonstrated by Borchers *et al.*<sup>1,2</sup> for Coulomb-excited  $2^+$  states in medium-heavy nuclei recoiling in iron. The gross systematic dependence of this field on atomic number and velocity (at which the ions enter the polarized medium) has been accounted for theoretically by Lindhard and Winther.<sup>3</sup> In this treatment the transient field is predominantly attributed to an enhancement of the electron spin density at the nucleus when polarized electrons are scattered in the ion potential.

As a tool for measuring nuclear magnetic moments, the transient field effect was first utilized in the case of  $^{54}\text{Fe}(2^+)$  by Hubler, Kugel, and Murnick.<sup>4</sup> The method was subsequently applied to  $s-d$  shell nuclei by the Utrecht group.<sup>5,6</sup>

The present work was motivated by the nuclear structure problem and also by the interest in the transient field, as a deviation from the Lindhard-Winther (LW) prediction with empirically adjusted parameters<sup>5,7</sup> was recently reported for oxygen in iron.<sup>8</sup> Possible sources for such behavior of the transient field were mentioned by LW<sup>3</sup> and recently emphasized in a review of the subject by Gelberg<sup>9</sup> at the Uppsala conference on hyperfine interactions (June, 1974).

### II. EXPERIMENTAL

Using the implantation perturbed-angular correlation (IPAC) method, the measurements were performed by determining the difference in pre-

cession angles when the excited nuclei are recoiled into magnetized iron and gold backings. As the observed effects were in the 1–5% range, the experimental setup and procedure will be described in some detail.

#### A. Setup

The nuclear levels studied were populated in the  $^{13,14}\text{C}({}^3\text{He}, p)^{15,16}\text{N}$  reactions, using  ${}^3\text{He}$  beams of 100–500 nA intensity from the Strasbourg 4 MV Van de Graaff accelerator, at energies of 3.1 and 3.8 MeV, respectively.

Carbon targets (50–80  $\mu\text{g}/\text{cm}^2$  thick) were deposited on sheets of gold (200  $\mu\text{m}$ ) and iron (25  $\mu\text{m}$ ) of the 99.99% purity grade manufactured by Goodfellow Metals Ltd. Self-supporting  $^{14}\text{C}$  targets ( $\approx 60\%$  enriched), prepared at Saclay by discharge cracking of methyl iodide, were floated onto the metal backings off the surface of an acetone-water mixture. The  $^{13}\text{C}$  targets (90% enriched) were vacuum-deposited onto the backings by electron bombardment. The measurements were performed using a number of iron backings. Annealing in hydrogen at  $\approx 700^\circ\text{C}$  improved the adhesion of the  $^{14}\text{C}$  foils under beam, but appeared to have no effect on the data (see Fig. 3).

The nuclear alignment and recoil energy were defined by observing  $\gamma$  rays in coincidence with back-flying protons. These were detected in a 500  $\mu\text{m}$  annular silicon counter (subtending lab angles of  $160^\circ < \theta_p < 170^\circ$ ) shielded from elastically scattered  ${}^3\text{He}$  and reaction  $\alpha$  particles by a 20  $\mu\text{m}$  gold mask. Consequently, the total counting rate was less than  $10^4$   $\text{s}^{-1}$  throughout. Examples of particles singles spectra are shown in Fig. 1(a).

The corresponding mean entrance velocities of the recoiling ions into the iron backing were  $v \approx 0.016(1)c$  for both nuclei, the error representing estimated target thickness broadening. The targets were secured perpendicular to the beam direction between the pole tips of a vertical electromagnet and subjected to a polarizing field of  $\approx 1.4$  kG. Four  $\gamma$  detectors were placed at angles close to the measured maximum slope of the angular correlations (one in each quadrant of the horizontal plane, see Fig. 2), at  $\theta_0 = 45^\circ$  for  $^{16}\text{N}$  (276 keV) and  $\theta_0 = 55^\circ$  for  $^{15}\text{N}$  (5.27 + 5.30 MeV).

For the  $^{16}\text{N}$  measurements Ge(Li) detectors were employed in order to resolve the 276 keV ( $1^- \rightarrow 0^-$ ) and 296 keV ( $3^- \rightarrow 2^-$ ) lines, as the protons leading to these excited states were not resolved. The coaxial detectors, varying in active volume between 20 and 40  $\text{cm}^3$ , were positioned at face distances of  $\approx 6$  cm from the target. For  $^{15}\text{N}$ , 12.7  $\times$  15.2 cm NaI(Tl) scintillators were used (face distance 20 cm), as the unresolved radiation from the neighboring  $\frac{1}{2}^+$  state at 5.30 MeV merely re-

duces the over-all anisotropy. Detailed angular correlations were measured for both nuclei, the results of which are summarized in Table II.

A conventional fast-slow coincidence system was used (time resolution  $\approx 5$  and 25 ns for NaI(Tl) and Ge(Li) counters, respectively). The coincident  $\gamma$ -energy pulses for all four detectors were mixed into a single analog-to-digital converter (ADC) and routed by logical identifier pulses into separate subsections of a 4096 channel analyzer.

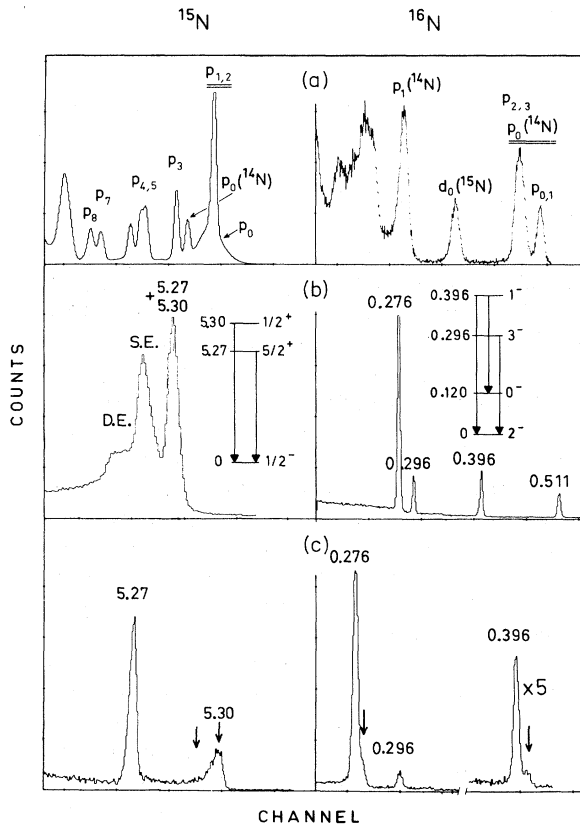


FIG. 1. (a) Examples of particle singles, (b)  $\gamma$  coincidence, and (c)  $0^\circ$  Ge(Li) spectra. All energies are in MeV. The underlined peaks in (a) correspond to the particle energy window settings. The arrows in (c) represent positions of Doppler-shifted peaks.

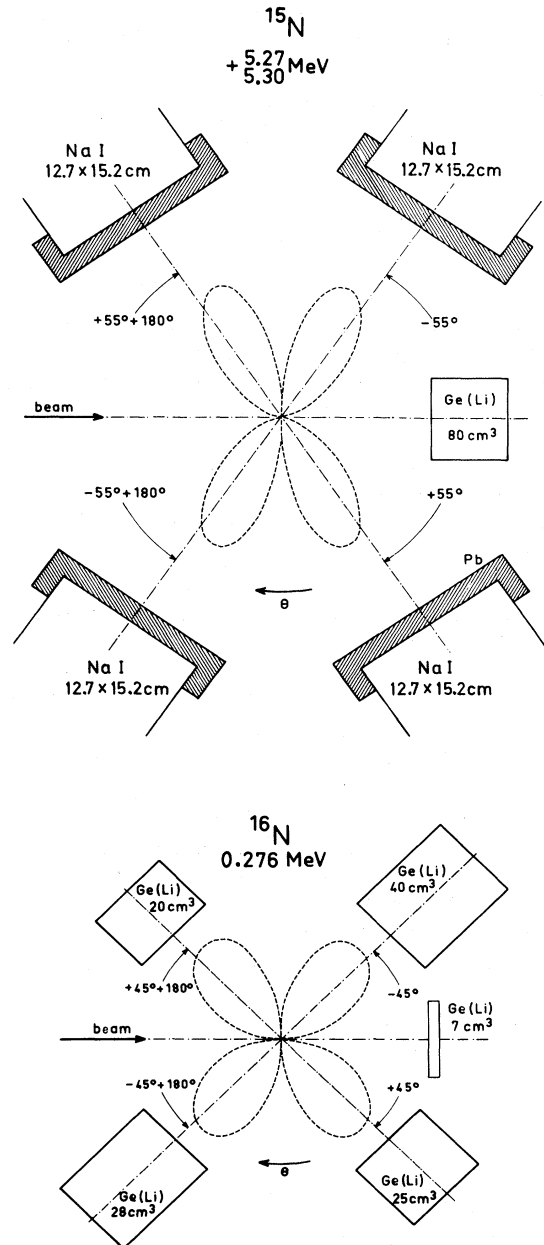


FIG. 2. Schematic display of the  $\gamma$  detector arrays. Also shown are polar plots of the measured  $|(1/W)dW/d\theta|$ .

An additional routing pulse was associated with the direction of the external magnetic field, which was reversed approximately twice a minute according to a preset number of counts in the particle energy window. As a precaution against faulty routing, the amplified gains were adjusted so that all photopeak positions of interest were staggered. The system was checked with all routing requirements operative at a total ADC counting rate of  $\approx 500 \text{ s}^{-1}$  with Ge(Li) singles spectra of a  $^{75}\text{Se}$  source. The maximum corresponding counting rate in coincidence was  $30 \text{ s}^{-1}$ . Examples of coincident  $\gamma$  spectra are presented in Fig. 1(b). The random coincidence fraction was in all cases less than 3% in the energy interval of interest.

In order to monitor the adhesion of the carbon layers to the backings throughout the measurements, an additional high-resolution Ge(Li) detector (7 cm<sup>3</sup> planar for  $^{16}\text{N}$  and 80 cm<sup>3</sup> coaxial for  $^{15}\text{N}$ ) at 0° to the beam registered coincident  $\gamma$ -ray spectra in a separate analyzer. The fraction of nuclei decaying in flight could be deter-

mined from the intensity of the Doppler-shifted  $\gamma$  peaks. Examples of 0° Ge(Li) spectra are shown in Fig. 1(c). The data acquisition took approximately three weeks for  $^{16}\text{N}$  and one week for  $^{15}\text{N}$ , during which gold and iron-backed targets were alternated. The data were dumped every eight hours or so. In analyzing the  $^{16}\text{N}$  results net photopeaks were integrated, whereas for  $^{15}\text{N}$  the single and double escape peaks were also included.

### B. Results and data handling

The relative change in counting rate with magnetic field is given, for small integral precession angles  $\Phi$ , by the expression

$$\epsilon \equiv \frac{N(\theta)_H - N(\theta)_{H=0}}{N(\theta)_{H=0}} = \Phi \left( -\frac{1}{W} \frac{dW}{d\theta} \right)_{\text{meas}}, \quad (1)$$

where  $W(\theta)$  represents the angular correlation.

With the angle convention of Fig. 2, the following expressions were formed from the measured counting rates, yielding  $\epsilon$  and two nonredundant

“null” effects to the same statistical significance:

$$\begin{aligned} \text{Quantity (a): } R_d &\equiv \frac{N(\theta_0) + N(\theta_0 + \pi)}{N(-\theta_0) + N(-\theta_0 + \pi)} \Bigg| \Bigg/ \frac{N(\theta_0) + N(\theta_0 + \pi)}{N(-\theta_0) + N(-\theta_0 + \pi)} \Bigg| = 1 + 4\epsilon, \\ \text{Quantity (b): } \text{Null}(1) &\equiv \frac{N(\theta_0) + N(-\theta_0)}{N(\theta_0 + \pi) + N(-\theta_0 + \pi)} \Bigg| \Bigg/ \frac{N(\theta_0) + N(-\theta_0)}{N(\theta_0 + \pi) + N(-\theta_0 + \pi)} \Bigg| = -1, \\ \text{Quantity (c): } \text{Null}(2) &\equiv \frac{N(\theta_0) + N(-\theta_0 + \pi)}{N(-\theta_0) + N(\theta_0 + \pi)} \Bigg| \Bigg/ \frac{N(\theta_0) + N(-\theta_0 + \pi)}{N(-\theta_0) + N(\theta_0 + \pi)} \Bigg| = -1. \end{aligned} \quad (2)$$

Quantities (b) and (c) reflect small field-correlated geometrical asymmetries; for example, (c) is sensitive to lateral beam displacement (to first order in the relative change in detector solid angle). These effects are, however, cancelled out to high order in (a), provided the detector efficiencies are well matched. As the individual Ge(Li) efficiencies spanned a factor of two (the NaI detectors were matched to within 20%), the quantities (a), (b), and (c) were also formed for the efficiency-normalized counting rates for each detector:

$$N_{\uparrow, \downarrow}^{\dagger} \equiv \frac{N_{\uparrow, \downarrow}}{N_{\uparrow} + N_{\downarrow}}.$$

In Fig. 3, efficiency-normalized double ratios [quantity (a)] are plotted in chronological order of data-taking for the transitions of major interest. In the  $^{16}\text{N}$  measurements the iron backings of targets III and IV were annealed in hydrogen, while those of targets I and II were not. All  $^{15}\text{N}$  data

were taken with annealed foils. Within statistics, there appear to be no systematic effects correlated with target history. The over-all averages of quantities (a), (b), and (c) evaluated for  $N$  and  $N^{\dagger}$  are presented in Table I for these transitions and for the  $^{16}\text{N}$  396 keV ( $1^- \rightarrow 2^-$ ) branch. For the subsequent analysis the efficiency-normalized values were adopted, although the two evaluation procedures yield results consistent to within a standard deviation. The Null(2) results are consistent with estimated beam displacements of the order of 5  $\mu\text{m}$ . Not surprisingly, the effects are more pronounced for the Ge(Li) detectors, as these were considerably closer to the target. One notes also that the recoil-in-gold measurements yield very small and consistent values for quantity (a) in all cases, as do the data for the essentially isotropic 396 keV transition.

The contact between the  $^{14}\text{C}$  targets and the backings deteriorated steadily when the beam current exceeded  $\approx 200 \text{ nA}$ . This was evident from an increase in the Doppler-shifted component of the

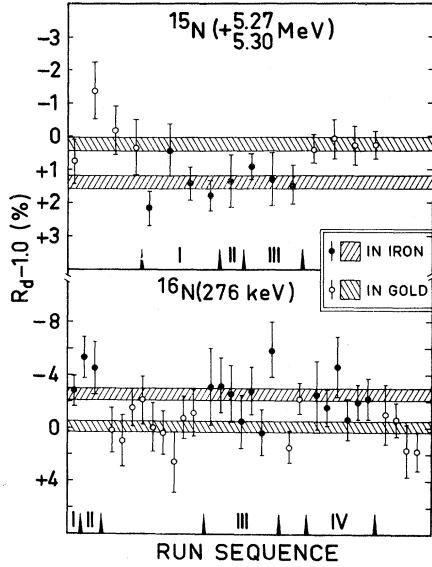


FIG. 3. The efficiency-normalized double ratios (see text) plotted in chronological order of measurement. Roman numerals label different iron-backed targets. Hatched areas represent over-all averages of the data.

276-296 keV lines in the  $0^\circ$  Ge(Li) spectra. The relative intensity of this component was identified with the fraction  $\eta$  of nuclei which decay outside the ferromagnet and hence do not experience precession. Whenever this fraction exceeded 5%, the iron-backed targets were changed and the corresponding data disregarded (the spectrum shown in Fig. 1(c) represents a poor target in this respect), and the following correction applied to the data run by run:

$$\epsilon_{Fe} = \frac{\epsilon_{Fe}^{exp} - \epsilon_{Au}^{exp}}{1 - \eta},$$

where the over-all average of the recoil-in-gold data  $\overline{\epsilon_{Au}^{exp}}$  is taken to represent the beam turning and associated effects. To first order in  $\eta$ , there are no other corrections to be applied, since the angular correlation of the 276 keV transition is attenuated very little when the nuclei recoil in vacuum at this velocity [ $G_2^{exp} = 0.915(15)$  (Ref. 10)]. No loss of contact was observed in the  $^{15}\text{N}$  measurements, presumably due to the superior method of target deposition. The measured precession angles  $\Phi$  and related quantities entering into Eq. (1) are summarized in Table II.

### III. INTERPRETATION PROCEDURE

As the  $g$  factor of the  $^{16}\text{N}(1^-)$  state has been determined,<sup>10, 11</sup> the precession data on this level can serve to calibrate the transient field at nitrogen nuclei. The measurement on  $^{15}\text{N}(\frac{5}{2}^+)$  can then yield the magnetic moment of the state. In this approach, the Lindhard-Winther theory<sup>3</sup> is only invoked in correcting the effective field for the nuclear lifetime dependence:

$$\tau_{^{16}\text{N}(1^-)} = 7.0(5) \text{ ps}$$

$$\tau_{^{15}\text{N}(\frac{5}{2}^+)} = 2.6(2) \text{ ps},$$

where  $\tau_{^{16}\text{N}(1^-)}$  is the adopted average of Refs. 11 and 12, and  $\tau_{^{15}\text{N}(\frac{5}{2}^+)}$  is the adopted average of four measurements quoted in Refs. 13 and 14 and confirmed by a Doppler shift attenuation method (DSAM) analysis of the  $0^\circ$  Ge(Li) spectra of the present work. Following Ref. 7, this correction factor was evaluated with the set of parameters which reproduce the systematics of transient field data to date. The results of this computation are

TABLE I. Summary of measured quantities. All values are in %. The lower of each pair of numbers is evaluated for efficiency-normalized counting rates (defined in text).

Nucleus	Transition	Quantity (a) 4 $\epsilon$		Quantity (b) Null (1)		Quantity (c) Null (2)	
		Iron	Gold	Iron	Gold	Iron	Gold
$^{16}\text{N}$	276 keV ( $1^- \rightarrow 0^-$ )	-2.58	+0.13	+0.42	-0.77	-0.14	+1.34
		(44)	(41)	(43)	(42)	(43)	(42)
		-2.54	-0.12	+0.07	-0.54	+0.33	+1.24
	396 keV ( $1^- \rightarrow 2^-$ )	-0.18	+0.37	+0.67	-0.06	-0.08	-1.27
(88)		(88)	(87)	(88)	(88)	(87)	
		-0.16	+0.46	+0.20	-0.11	0.00	-1.23
$^{15}\text{N}$	+5.27 MeV 5.30 MeV	+1.38	+0.28	-0.11	+0.44	+0.15	-0.02
		(20)	(20)	(20)	(20)	(20)	(20)
	$\left( \begin{array}{c} \frac{5}{2}^+ \rightarrow \frac{1}{2}^- \\ \frac{1}{2}^+ \rightarrow \frac{3}{2}^- \end{array} \right)$	+1.39	+0.23	-0.16	+0.43	+0.01	+0.02

TABLE II. Measured precessions and related quantities.

Nucleus	Transition	$\overline{\epsilon}_{\text{Fe}}$	Angular correlation coefficients	$-\frac{1}{W} \frac{dW}{d\theta}(\theta_0)$	$\Phi_{\text{net}}(\text{Fe})$ (mrad)
$^{16}\text{N}$	276 keV ( $1^- \rightarrow 0^-$ )	-0.0063(13)	$A_2 = 0.336(13)$	+0.464(17)	-13.6(2.7)
	296 keV ( $3^- \rightarrow 2^-$ )	-0.0020(40)	$A_2 = -0.173(34)$ $A_4 = 0.110(36)$	-0.209(63)	+10(19) -28(19) <sup>a</sup> } -9(13)
	396 keV ( $1^- \rightarrow 2^-$ )	-0.0016(31)	$A_2 = 0.02(2)$ $A_4 = 0.00(2)$	+0.027(35)	-59(13.7)
$^{15}\text{N}$	+5.27 +5.30 MeV $\left( \begin{array}{c} \frac{5}{2}^+ \rightarrow \frac{1}{2}^- \\ \frac{1}{2}^+ \rightarrow \frac{1}{2}^- \end{array} \right)$	+0.0028(7)	$A_2 = 0.325(12)$ $A_4 = -0.096(15)$	+0.519(19)	+5.6(1.4)

<sup>a</sup> From a preliminary measurement at 2.1 MeV bombarding energy.

displayed in Fig. 4 and one deduces

$$\frac{\Phi/g(^{15}\text{N}_{5/2^+})}{\Phi/g(^{16}\text{N}_{1^-})} = 0.83(5).$$

The quoted error stems principally from the uncertainties in the time parameters  $t_s$  ( $\approx 0.7$  ps) and  $\tau_{\text{nucl}}$ , which characterize the transient field precession. In this context one notes that the assumed coefficient of electronic stopping power (of  $0.9k_e$ , relative to the Lindhard-Scharff-Schiøtt theory<sup>15</sup>) is consistent with the results of recent systematics by Broude *et al.* on  $^{22}\text{Ne}$  ions slowing down in diverse backings.<sup>16</sup>

With the values of the net precession angles of the nuclear spin  $\Phi_{\text{net}}(\text{Fe})$  of Table II and adopting<sup>10, 11</sup>

$$|g(^{16}\text{N}_{1^-})| = 1.82(14),$$

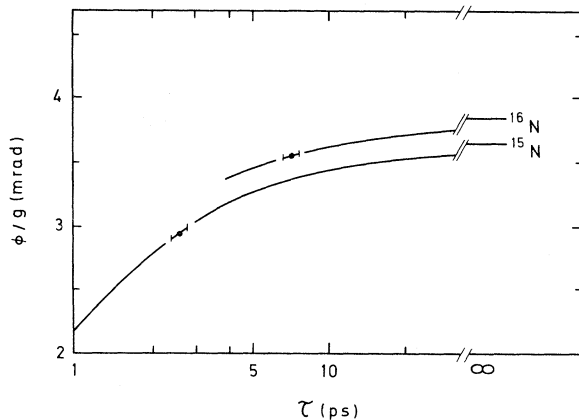


FIG. 4. Calculated transient field precession angles as a function of nuclear lifetime for the ion energies of the present work. The time intervals indicate adopted values of  $\tau_{\text{nucl}}$  for the levels involved.

we obtain (a) a negative spin for this  $g$  factor, (b)  $g(^{15}\text{N}_{5/2^+}) = +0.9(3)$ , and (c) a value for the transient field which is enhanced with respect to the empirically adjusted LW prediction<sup>7</sup> by

$$F \equiv \frac{\Phi_{\text{meas}}}{\Phi_{\text{calc}}} = 2.1(5).$$

Lowering the cutoff ion energy from 5 keV to 1 keV<sup>5</sup> would imply a reduction in  $F$  of about 10%. Recoil velocity uncertainty due to target thickness affects the results by less than 3%.

#### IV. DISCUSSION

It is implicit in the analysis of the previous section that there is no contribution to the precession from static fields. These fields at nitrogen in iron are not known and the information on light ( $Z < 20$ ) impurities in solids is, in general, rather scant. However, the measured fields at boron,<sup>17</sup> fluorine,<sup>18</sup> aluminum,<sup>19</sup> and phosphorous<sup>20</sup> in iron are all smaller (in absolute magnitude) than 100 kG, in contrast to heavier impurity elements where megagauss fields are encountered.<sup>21</sup>

With respect to the  $^{15}\text{N}(\frac{5}{2}^+)$   $g$  factor, a static field as large as 100 kG (in absolute magnitude), which is evidently a reasonable upper limit, would affect the deduced value by less than one quoted standard deviation. In contrast,  $H_{\text{static}} = 100$  kG would account for about half the observed precession of the  $^{16}\text{N}(1^-)$  state, due to its longer lifetime. However, there are indications that the static field is considerably below this limit. These are: An IPAC measurement has yielded a very low limit on the magnitude of the static field at boron nuclei in iron<sup>17</sup>:

$$-1.6 \text{ kG} < H_{\text{static}} < +3.9 \text{ kG}.$$

It is probable that this very low field is associated with interstitial locations in the *bcc* lattice, as shown by the Tokyo group in nuclear magnetic resonance measurements on the  $\beta$  emitters  $^{12}\text{B}$  and  $^{12}\text{N}$  implanted in a series of *bcc* metallic hosts (Nb, Mo, Ta, W).<sup>22</sup> Moreover, time-differential IPAC measurements have clearly demonstrated that the fields at fluorine nuclei occupying interstitial locations in iron are a factor of 2 to 3 smaller than at a substitutional site.<sup>18</sup>

The existence of an enhancement in the transient field of nitrogen depends (apart from the statistical significance) on the assumption that the static field is reduced below the 100 kG limit by a comparable factor. However, the deduced enhancement factor of

$$F(\text{nitrogen}) = 2.1(5)$$

is in good agreement with one recently found for oxygen, of<sup>8</sup>

$$F(\text{oxygen}) = 2.2(5).$$

In this context it is noteworthy that the  $^{18}\text{O}(2_1^+)$  state, on which that measurement was performed, has a lifetime shorter by a factor of 2.5 than that of the  $^{16}\text{N}(1^-)$  state. Possible sources for such enhancements were discussed in the original LW paper,<sup>3</sup> and might be due to capture of polarized electrons in bound *s* states of the moving ion, as recently reemphasized by Gelberg.<sup>9</sup>

The mass-15 nuclei have been extensively studied theoretically<sup>23-28</sup> and experimentally,<sup>13, 29-34</sup> In particular, the wave functions of the  $\frac{5}{2}^+$  states at about 5.2 MeV excitation in these nuclei have been assigned predominantly  $(p_{1/2})^{-2}(d_{5/2})^1$  and  $(p_{1/2})^{-4}(s, d)^3$  components. A pure configuration

of the former type would imply

$$g_{\text{calc}} = +1.03,$$

whereas the latter would suggest a value for  $g$  close to that of the  $^{19}\text{F}(\frac{5}{2}^+)$  state at 0.198 MeV, for which

$$g(^{19}\text{F}_{5/2^+})_{\text{meas}} = +1.44.$$

An alternative description<sup>29</sup> is based on similarities in  $\alpha$  scattering on  $^{15}\text{N}$ ,  $^{16}\text{O}$ , and the considerably enhanced ( $\frac{3}{2}^+ \rightarrow \text{g.s.}$ ) and ( $3^- \rightarrow \text{g.s.}$ ) *E3* transitions in these respective nuclei.<sup>13</sup> In this picture, the level under study has been assigned a large  $\pi(p_{1/2})^{-1} \otimes ^{16}\text{O}(3^-)$  component. Taking the Schmidt value for a  $p_{1/2}$  proton and the experimental value<sup>35,36</sup>  $|g(^{16}\text{O}_{3^-})| = 0.55$  (the sign is assumed positive), one expects

$$g_{\text{calc}} = +0.7$$

for a pure configuration of this type.

#### ACKNOWLEDGMENTS

The authors would like to express their gratitude to Professor I. Talmi for his helpful comments. The assistance of Dr. Bianchi of Saclay in preparing the  $^{14}\text{C}$  targets and of Mr. F. Kuntz in constructing the mechanical assembly is greatly appreciated. Three of us (M.B.G., K.-H.S., and P.N.T.) would like to thank Professor R. Armbruster and the staff of the Centre de Recherches Nucléaires for their hospitality and assistance. One of us (P.N.T.) is indebted to Professor E. Bodenstedt for a visiting fellowship to the Institut für Strahlen-und Kernphysik, Bonn.

\*On leave from the Weizmann Institute of Science, Rehovot, Israel.

†On leave from the Tata Institute of Fundamental Research, Bombay, India.

<sup>1</sup>B. Herskind, R. R. Borchers, J. Bronson, D. E. Murnick, L. Grodzins, and R. Kalish, in *Hyperfine Structure and Nuclear Radiations*, edited by E. Matthias and D. A. Shirley (North-Holland, Amsterdam, American Elsevier, New York, 1968), p. 735.

<sup>2</sup>R. R. Borchers, B. Herskind, J. Bronson, L. Grodzins, R. Kalish, and D. E. Murnick, *Phys. Rev. Lett.* **20**, 424 (1968).

<sup>3</sup>J. Lindhard and A. Winther, *Nucl. Phys.* **A166**, 413 (1971).

<sup>4</sup>G. K. Hübner, H. W. Kugel, and D. E. Murnick, *Phys. Rev. Lett.* **29**, 662 (1972).

<sup>5</sup>J. L. Eberhardt, R. E. Horstman, H. W. Heeman, and G. van Middelkoop, *Nucl. Phys.* **A229**, 162 (1974).

<sup>6</sup>R. E. Horstman, J. L. Eberhardt, H. A. Doubt, and

G. van Middelkoop, in *Proceedings of the International Conference on Nuclear Structure and Spectroscopy, Amsterdam, 1974*, edited by H. P. Blok and A. E. L. Dieperink (Scholar's Press, Amsterdam, 1974), Vol. II, p. 136.

<sup>7</sup>G. K. Hübner, H. W. Kugel, and D. E. Murnick, *Phys. Rev. C* **9**, 1954 (1974).

<sup>8</sup>M. Forterre, J. Gerber, J. P. Vivien, M. B. Goldberg, and K.-H. Speidel, *Phys. Lett.* **55B**, 56 (1975).

<sup>9</sup>A. Gelberg, *Phys. Scr.* (to be published).

<sup>10</sup>M. Forterre, J. Gerber, J. P. Vivien, M. B. Goldberg, and K.-H. Speidel, in *Proceedings of the International Conference on Hyperfine Interactions Studied in Nuclear Reactions and Decay*, Uppsala, Sweden, 10 June 1974 (unpublished), p. 92.

<sup>11</sup>W. L. Randolph, J. Asher, J. R. Beene, N. Ayres de Campos, M. A. Grace, P. M. Rowe, D. F. H. Start, and N. Anyas Weiss, in *Proceedings of the International Conference on Hyperfine Interactions Studied in Nuclear*

- Reactions and Decay, Uppsala, Sweden, 10 June 1974 (see Ref. 10), p. 90.
- <sup>12</sup>M. Forterre, J. Gerber, J. P. Vivien, M. B. Goldberg, and K.-H. Speidel, in *Proceedings of the International Conference on Nuclear Structure and Spectroscopy, Amsterdam, 1974* (see Ref. 6), p. 123.
- <sup>13</sup>R. D. Gill, J. S. Lopes, B. C. Robertson, R. A. I. Bell, and H. J. Rose, *Nucl. Phys.* **A106**, 678 (1968).
- <sup>14</sup>E. B. Dally, M. G. Croissiaux, and B. Schweitz, *Phys. Rev. C* **2**, 2057 (1970).
- <sup>15</sup>J. Lindhard, M. Scharff, and H. E. Schiøtt, K. Dan. Vidensk. Selsk. Mat. Fys.-Medd. **36**, No. 14, 1 (1963).
- <sup>16</sup>C. Broude, P. Engelstein, M. Popp, and P. N. Tandon, *Phys. Lett.* **39B**, 185 (1972).
- <sup>17</sup>R. Avida, I. Ben-Zvi, G. Goldring, S. S. Hanna, P. N. Tandon, and Y. Wolfson, *Nucl. Phys.* **A182**, 359 (1972).
- <sup>18</sup>J. Braunsfurth, J. Morgenstern, H. Schmidt, and H. J. Körner, *Z. Phys.* **202**, 321 (1967); R. G. Stokstad, R. A. Moline, C. A. Barnes, F. Boehm, and A. Winther, in *Hyperfine Structure and Nuclear Radiations* (see Ref. 1), p. 699.
- <sup>19</sup>M. Kontani and J. Itoh, *J. Phys. Soc. Jpn.* **22**, 345 (1967).
- <sup>20</sup>E. Koster and B. G. Turrell, *J. Appl. Phys.* **42**, 1314 (1971).
- <sup>21</sup>See, e.g., R. R. Borchers, in *Hyperfine Interactions in Excited Nuclei*, edited by G. Goldring and R. Kalish (Gordon and Breach, London, 1971), p. 31.
- <sup>22</sup>T. Minamisono, K. Matuda, A. Mizobuchi, and K. Sugimoto, *J. Phys. Soc. Jpn.* **30**, 311 (1971).
- <sup>23</sup>E. C. Halbert and J. B. French, *Phys. Rev.* **105**, 1563 (1957).
- <sup>24</sup>D. Kurath, *Nucl. Phys.* **73**, 1 (1965).
- <sup>25</sup>A. P. Zuker, B. Buck, and J. B. McGrory, *Phys. Rev. Lett.* **21**, 39 (1968).
- <sup>26</sup>A. P. Shukla and G. E. Brown, *Nucl. Phys.* **A112**, 296 (1968).
- <sup>27</sup>S. Lie, T. Engeland, and G. Dahll, *Nucl. Phys.* **A156**, 449 (1970).
- <sup>28</sup>B. S. Reehal and B. H. Wildenthal, *Particles and Nuclei* **6**, Nos. 5-6, 137 (1973).
- <sup>29</sup>A. Bussiere, N. K. Glendenning, B. G. Harvey, J. Mahoney, J. R. Meriwether, and D. J. Horen, *Phys. Lett.* **16**, 296 (1965).
- <sup>30</sup>E. K. Warburton, J. W. Olness, and D. Alburger, *Phys. Rev.* **140**, B1202 (1965).
- <sup>31</sup>S. Gorodetzky, R. M. Freeman, A. Gallmann, and F. Haas, *Phys. Rev.* **149**, 801 (1966).
- <sup>32</sup>J. S. Lopes, O. Häusser, H. J. Rose, A. R. Poletti, and M. F. Thomas, *Nucl. Phys.* **76**, 223 (1966).
- <sup>33</sup>W. P. Alford and K. H. Purser, *Nucl. Phys.* **A132**, 86 (1969).
- <sup>34</sup>R. Avida, M. B. Goldberg, Y. Horowitz, K.-H. Speidel, and Y. Wolfson, *Nucl. Phys.* **A172**, 113 (1971).
- <sup>35</sup>W. L. Randolph, N. Ayres de Campos, J. R. Beene, J. Burde, M. A. Grace, D. F. H. Start, and R. E. Warner, *Phys. Lett.* **44B**, 36 (1973).
- <sup>36</sup>C. Broude, M. B. Goldberg, G. Goldring, M. Hass, M. J. Renan, B. Sharon, Z. Shkedi, and D. F. H. Start, *Nucl. Phys.* **A215**, 617 (1973).